Observation of resistive Weibel instability in intense laser plasma

S. Krishnamurthy, K. Makur and B. Ramakrishna [ID]

Department of Physics, Indian Institute of Technology Hyderabad, Sangareddy, Telangana 502285, India

Abstract

We observe experimentally periodic proton beam filamentation in laser-produced dense plasma using multilayered (CH–Al–CH) sandwich targets. The accelerated MeV proton beams from these targets exhibit periodic frozen filaments up to 5–10 μm as a result of resistive Weibel instabilities in the expanding plasma. The evolution of strong self-generated resistive magnetic fields at the targets interface is attributed to such plasma effects, which are supported, by our theory and simulations. We suggest that the resistive Weibel instability could be effectively employed to understand the evolution of magnetic fields in laser-generated plasma in the astrophysics scenario or the advanced fast igniter approach of the inertial confinement fusion.

Introduction

Remarkable progress in the field of intense laser-matter interaction has been witnessed with the advent of a chirped pulse amplification (CPA) technique (Strickland and Mourou, 1985). Laser-driven ion acceleration is immensely important as it has the potential to overcome the barrier faced by conventional accelerators. Amongst target normal sheath cceleration (TNSA), radiation pressure acceleration (RPA), collisionless shock acceleration (CSA), and other mechanisms of laser-driven ion acceleration, TNSA is the most widely accepted mechanism (Mora, 2003), in which the laser pulse ionizes the front surface of the target and the electrons acquire energy from the peak of the pulse, these electrons are termed as fast electrons as they have higher kinetic energy. Fast electrons advance through the material and extend into the vacuum thereby creating a charge separation leading to a sheath electric field, which accelerates the ions in the vicinity. The accelerated ion energies are therefore dependent on the fast electrons. In addition to ion acceleration, the laser-generated fast electrons and their propagation in the target medium are important in various other applications, such as fast ignition in inertial confinement fusion (ICF) (Craxton *et al.*, 2015; Betti and Hurricane, 2016), generation of X rays (Gahn *et al.*, 1998; Norreys *et al.*, 1999; Yu *et al.*, 1999; Ledingham *et al.*, 2000), γ rays (Cowan *et al.*, 1999; Gahn *et al.*, 2000; Chen *et al.*, 2009), and positrons (Clark *et al.*, 2000; Maksimchuk *et al.*, 2000; Snavely *et al.*, 2000). When fast electrons propagate in a dense solid target, the return cold electron currents are setup so that the requirement of charge neutrality is fulfilled in the plasma. Equilibrium between fast electrons and return electrons are unstable due to electromagnetic perturbation leading to Weibel instability, which produces strong filamentation of the fast electron beam. The efficiency of energy transport becomes very poor and intense fast electrons cannot transport beyond the filament length (Bell and Kingham, 2003). Instabilities have been modeled by connecting collisional and collisionless plasmas (Bret, 2010) and also by considering quantum effects in the pre-compressed target (Bret *et al.*, 2009) in order to understand the effects on the energy transfer from beam to pellet in the fast ignition scenario.

   TNSA yields polyenergetic ions because the ions are accelerated by the sheath electric field, which is Gaussian in shape. The divergence of laser-accelerated protons (10–30°) is also set depending on the energy of the accelerated beam. Efforts have been made to gain control over the ion beam profile by employing a photoresist (PR) (Metzkes *et al.*, 2014), hydrocarbon (CH) layer (Ramakrishna *et al.*, 2015) on the rear surface of the target in order to reduce the transverse modulations in the ion beam. In a multilayered target, the material boundary will cause a change in resistivity, which affects the magnetic field generation, and growth thereby affecting the flow of electrons as described in the theoretical work (Robinson and Sherlock, 2007) and a proof-of-principle experiment (Ramakrishna *et al.*, 2010). Other methods like using a shaped target, quadrupole magnets, and compact ion lens driven by a secondary laser beam have been attempted to achieve geometrical focusing of the laser-driven protons (Toncian *et al.*, 2006; Kar *et al.*, 2008, 2011; Nishiuchi *et al.*, 2009). Since the typical laser to proton conversion efficiency previously reported from many experiments is less than 10% (Fuchs *et al.*, 2006; Robson *et al.*, 2006), it is crucial to maintain maximum proton flux for various applications, including hadron therapy and fast ignition. In the fast ignition
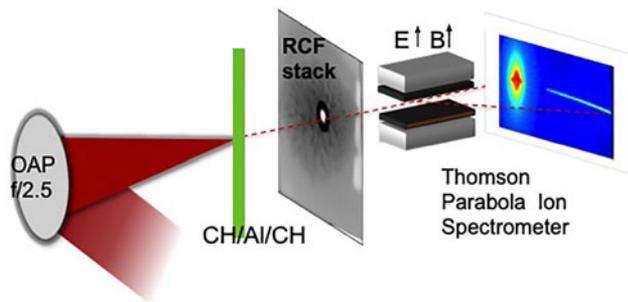
Fig. 1. (Color online): A schematic diagram of the experimental setup showing the RCF position behind the target.

approach, some proposals are currently being investigated to use proton beams in addition to the fast electrons to heat the core of the imploding capsule using CH layered targets. This design can reduce the core arrival time lags due to different ion energies, and ion beams with wide energy spectra can be accepted (Sakagami *et al.*, 2016). However, the plasma instabilities affect the energy and beam profile of the ions and understanding such filamentary effects in proton beam is important that is otherwise proven to be detrimental for ICF.

Experimental details

The experiment was carried out at HZDR, Dresden, using the 150 TW Ti:sapphire laser system delivering 30 fs (FWHM) at 10 Hz repetition rate, at a central wavelength of 800 nm. The *p*-polarized laser beam was focused to a focal spot of 8 μm diameter (FWHM) with an off-axis parabolic mirror with a focal length of 250 mm, reaching a peak intensity of the order of $\sim 3 \times 10^{20}$ W/cm^2 (Schramm *et al.*, 2017). The dispersed ion

beam was detected by a micro-channel plate (MCP) detector coupled to a 16-bit camera. A stack of radiochromic films (RCFs) was placed at 5 cm behind the target to detect the ion beam profile. RCF was used because it is an absolutely calibrated dosimetry medium, which changes its color on exposure to ionizing radiation. Protons of a given energy will traverse only through a well-defined thickness of the film before depositing the energy at the Bragg peak (Xu *et al.*, 2019). Therefore, each layer of RCF stack could be associated with a definite minimum proton energy (Fig. 1).

Results and discussion

In this paper, we report the observation of proton beam filamentation at relativistic laser intensities. The filamentary structures observed in the proton beam are observed to uniformly evolve as the ultrafast (ps) plasma channel expands, which is clearly evidenced by the proton beam distribution recorded on each layer (6–10 MeV) of RCF stack as shown in Figure 2. The fast electron beam generated at the critical density surface of the plasma is observed to be divergent in the laser-plasma interaction (Santala *et al.*, 2000). Very large instantaneous currents (10^6–10^9 A) produced will lead to strong collective effects (Bell *et al.*, 1997; Davies *et al.*, 1997), which results in fine structure (i.e., filaments) (Bell and Kingham, 2003) and hence divergence of the beam. The target chosen for the present experiment is CH–Al–CH and Al–CH–Al multilayered targets. First, given the large resistivity expected in dielectric materials, plastic targets are ideal candidates to investigate the generation of resistive fields (Jung *et al.*, 2005). Second, using multilayers, it is possible to change the resistivity gradient, which can have a direct impact on the magnetic fields generated.

The theory behind collimation of fast electrons in a structured target could be understood by combining ohm's law with
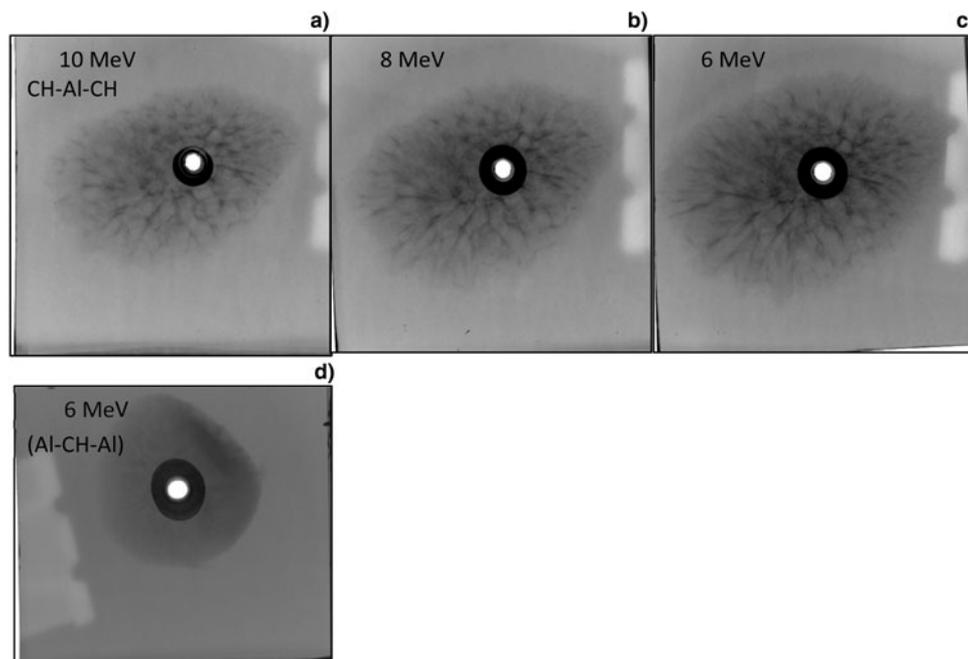
Fig. 2. (Color online): Proton beam profiles (a) 10 MeV, (b) 8 MeV, and (c) 6 MeV recorded on RCF from the target rear surface CH–Al–CH (2.5 μm); (d) shows a smooth beam recorded on RCF from the target rear surface of Al–CH–Al (2.5 μm).

Faraday's law for the growth rate of magnetic field resulting in the following equation:

$$\frac{\partial B}{\partial t} = \eta \nabla \times j + (\nabla \eta) \times j, \qquad (1)$$

where η is the resistivity and j is the fast electron current density. The first term corresponds to the magnetic fields that act to push fast electrons toward regions of higher fast electron density, while the second term corresponds to the magnetic fields that push the fast electrons toward regions of higher resistivity. The first term of Eq. (1) is the origin of electromagnetic instability. A fast electron current density perturbation normal to the streaming direction (i.e., normal to the direction of j) will generate the magnetic field that would push more fast electrons into the high density region from the low density region (the higher the density of fast electrons is, the higher the current density is: j). More and more fast electrons are constricted together, which further strengthens the density perturbation. Consequently, the generated field gets stronger further according to Eq. (1), and the density ripple magnitude gets larger and larger. As a result, the Weibel instability is created and filaments (a sequence of high and low density structures) are formed.

Figure 2a–2c shows filamentation in the proton beam imprint from the rear side of the CH–Al–CH target, as recorded on an RCF arising due to self-generated resistive instabilities (Sentoku *et al.*, 2000, 2011). Figure 2d represents the proton beam profile of a 6 MeV RCF observed from the Al–CH–Al target, which represents a smooth collimated beam with no net-like pattern. Robinson and Sherlock (2007) have highlighted the potential for harnessing these self-generated fields for guided electron beam transport in targets specifically designed to give rapid magnetic field growth at a well-defined boundary.

The divergence of the beam calculated for the CH–Al–CH foil is around 30° calculated from the recorded RCF data. The common inference from these figures is that whenever a low-Z thin transport layer is present on the rear side, we can observe a filamented proton beam imprint on the RCF. Similar experiments were conducted on the HZDR DRACO Laser facility using thin foil titanium (Ti) targets (2 and 3 μm), wherein they have reported transverse modulations in the proton beam profile (Metzkes *et al.*, 2014). They have used a very thick hydrocarbon transport layer (3.5 μm) at the rear side of 2-μm Ti foil to control the spatial modulations in the beam. In this experiment, we have used the advantage of inherent resistivity gradient of the targets to control the filamentation without increasing the thickness of the rear side transport layer.

Figure 3a represents the magnified proton beam profile, which depicts an increasingly strong modulation for thinner targets. Particularly, striking is the profile which exhibits a high-contrast modulation with an elaborate net-like periodic uniform structure. Inspection of consecutive films illustrates that the structure persists deep into the stack with almost constant formation, indicating that it is formed well in advance of the detector surface. Also, the filamentary structures are constantly present in all ranges of energy as shown in Figure 2a–2c, indicating that the filamentation has occurred well inside the target with the fast electrons and the corresponding structure is mapped onto the protons through the sheath electric field.

The typical structure size at the stack is 0.2 cm over a beam that extends 5 cm on the stack. Assuming a beam originating from a radial size of 100–200 μm (Borghesi *et al.*, 2004) and that the
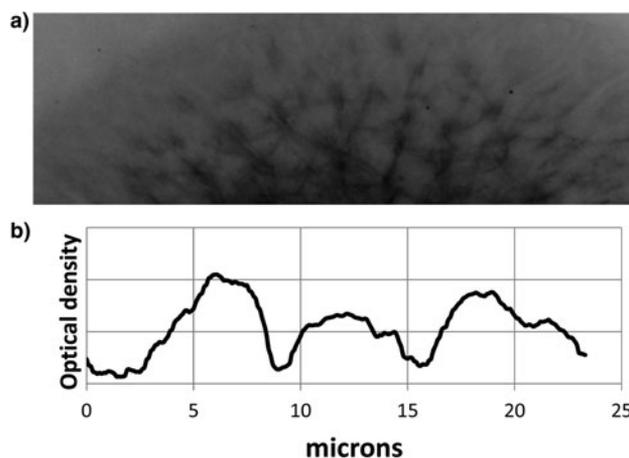
Fig. 3. (a) A zoom in the profile depicting a net-like pattern in the proton beam imprint. (b) A line out of the pattern shows periodicity in the net pattern.

expansion of the structure is ballistic from the target surface where it was generated to the detector, implies an instability wavelength, of 6–8 μm or less. This is greater than the typical wavelength of surface modulations on the foils, which is about 0.1 μm. We have further investigated the mechanism for the filamentation of the beam observed in the experiment. Resistivity (Gremillet *et al.*, 2002; Debayle and Tikhonchuk, 2008; Robinson *et al.*, 2008), ionization (Krasheninnikov *et al.*, 2005), and Weibel (Fried, 1959; Weibel, 1959; Grassi *et al.*, 2017) instabilities are typically invoked to explain the filamentation of fast currents observed experimentally (Borghesi *et al.*, 1999; Gremillet *et al.*, 1999; Tatarakis *et al.*, 2003; Wei *et al.*, 2004). In physical terms, resistive filamentation occurs because any transverse perturbation in the current density will resistively grow a magnetic field that drives fast electrons into the perturbation. As this increases the local current density, the magnetic field gets further enhanced and a positive feedback is created. Our experimental observation that the filamentation wavelength $\lambda = 2\pi/k = 6$–8 μm agrees well with the reported wavelength for Weibel instability to be about 5–15 μm (Romagnani *et al.*, 2019) using the proton probe technique. From our observations, we conclude that Weibel instabilities at faster time scales may be the root cause to seed resistive instabilities in the target leading to the filamentation.

PIC simulations

To investigate the filamentation and corresponding correlation to the divergence of the proton beam from sandwich targets, 2D particle-in-cell (PIC) simulation was carried out using the EPOCH (Arber *et al.*, 2015). The simulation domain was chosen to be 40 μm × 40 μm along x- and y-directions with a grid resolution of 20 nm along each direction accommodating 32 macroparticles per cell. The laser pulse of duration 30 fs, wavelength 0.8 μm propagates along the positive x-direction with a transverse Gaussian profile. The laser focal spot and intensity were taken to be 8 μm and 3×10^{20} W/cm^2 in accordance with the parameters used during the experiment. The simulations were carried out for sandwich targets Al–CH–Al (1–0.5–1 μm) and CH–Al–CH (1–0.5–1 μm) with $n_{Al} = 10n_c$, and for the plastic CH layer, we assumed $n_{carbon} = 10n_c$, $n_H = 20n_c$, where $n_c = 1.74 \times 10^{21}$ cm^{-3}. Both the targets were coated with a 50 nm proton
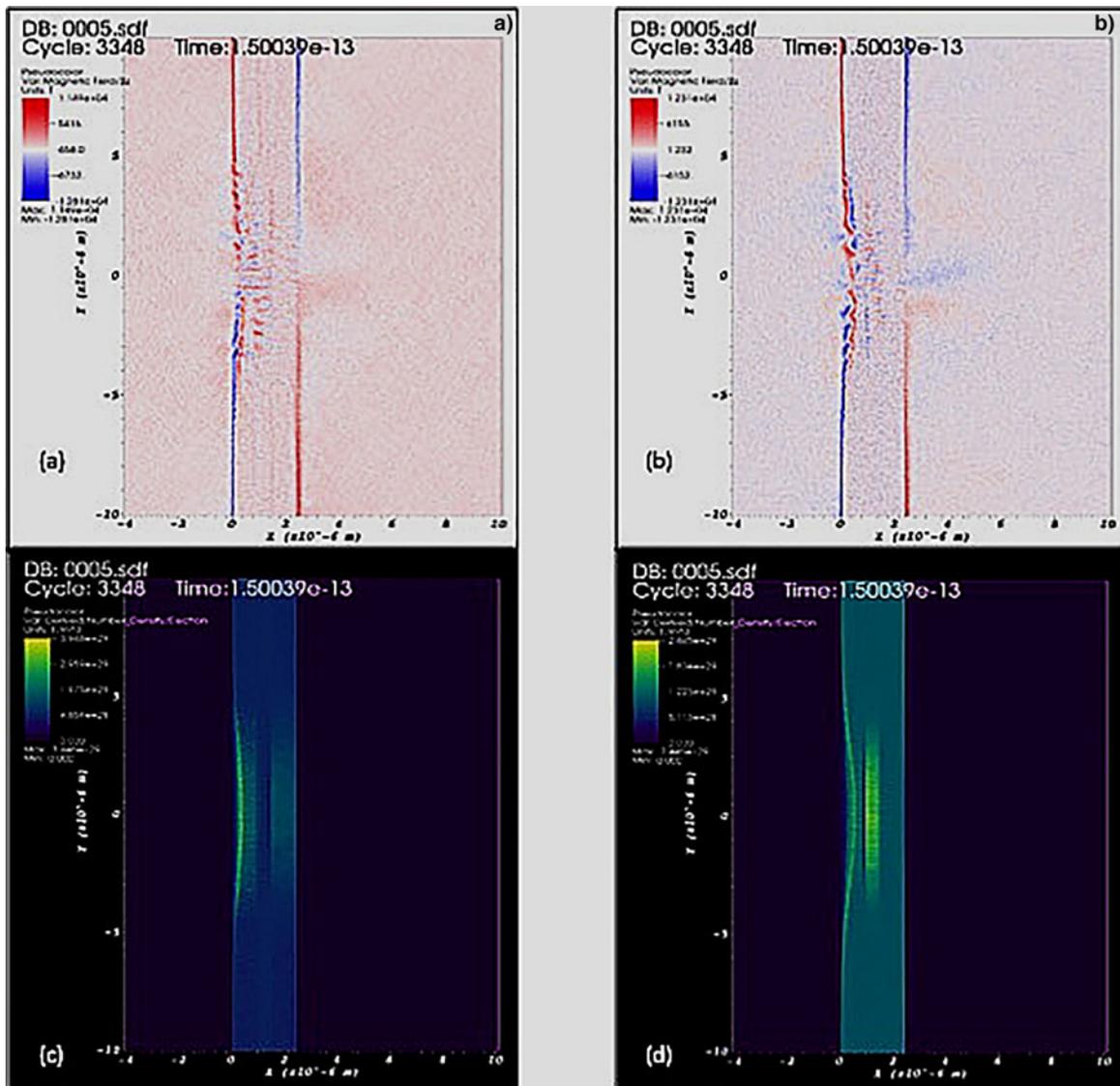
Fig. 4. Magnetic field within the target for (a) Al–CH–Al and (b) CH–Al–CH. The electron number density within the target for (c) Al–CH–Al and (d) CH–Al–CH.

layer on the rear side in order to account for the effect of contaminant layer in the experiment, structures of fast electrons are mapped on to the sheath electric field, which is directly correlated to the acceleration of protons. Therefore, protons accelerated from the rear side of the target would also exhibit filamentation as observed from the experiment.

Figure 4a represents that the magnetic field inside Al–CH–Al cease to grow once the modulations reach the boundary of the interface between CH–Al layers on the rear side, and therefore, the modulations are not propagated through to the rear surface of the target. Whereas in case of CH–Al–CH (Fig. 4b), it can be clearly seen that the filaments do not get suppressed near the boundary of the rear side layers and propagate through to the rear surface of the target. Similarly, the number density of electrons in Al–CH–Al (Fig. 4c) do not show filamentary structures in the layer corresponding to the rear side of the target, but CH–Al–CH (Fig. 4d) clearly has the filamentary structure in the layer at the rear side of the target. These filamentary structures of fast electrons are mapped on to the sheath electric field,

which is directly correlated to the acceleration of protons. Therefore, protons accelerated from the rear side of the target would also exhibit filamentation as observed from the experiment.

The parameter, which indicates the divergence of the proton beam, is the spread in the transverse momentum P_y of the protons. The spread in the transverse momentum P_y is measured at $P_x = 20 \times 10^{-21}$ kg m/s for both the targets. Al–CH–Al (Fig. 5a) has a spread of 2.98×10^{-21} kg m/s, whereas CH–Al–CH (Fig. 5b) has a spread of 4.11×10^{-21} kg m/s, indicating that the protons from CH–Al–CH are more divergent than that from Al–CH–Al as observed from the experiment. The histogram of the electric field over the entire simulation domain is shown in Figure 6. The maximum value of the sheath electric field reached for Al–CH–Al is about 10 TV/m, whereas for CH–Al–CH, the maximum is about 6 TV/m. This implies that the formation of filamentary structures inside the target rear surface may have caused perturbation in the sheath field and, therefore, may have direct correlation in the observed reduction in the sheath electric field for the target CH–Al–CH.

Fig. 5. The phase space distribution of protons at 1ps for (a) Al–CH–Al and (b) CH–Al–CH.

Fig. 6. A histogram of the electric field for both the targets.

astrophysical scenario (Cassam-Chenai *et al.*, 2008; Suzuki-Vidal, 2015), that is, when a supernova collapses to form a neutron star a similar counter streaming charged particles may give rise to instability leading to generation of strong magnetic field. Charged particles streaming in such high magnetic fields may also contribute to gamma ray bursts.

References

Arber TD, Bennett K, Brady CS, Lawrence-Douglas A, Ramsay MG, Sircombe NJ, Gillies P, Evans RG, Schmitz H, Bell AR and Ridgers CP (2015) Contemporary particle-in-cell approach to laser-plasma modelling. *Plasma Physics and Controlled Fusion* **57**, 113001.

Bell AR and Kingham RJ (2003) Resistive collimation of electron beams in laser-produced plasmas. *Physical Review Letters* **91**, 035003.

Bell AR, Davies JR, Guerin S and Ruhl H (1997) Fast-electron transport in high-intensity short-pulse laser-solid experiments. *Plasma Physics and Controlled Fusion* **39**, 653.

Betti R and Hurricane OA (2016) Inertial-confinement fusion with lasers. *Nature Physics* **12**, 435.

Borghesi M, Mackinnon AJ, Bell AR, Malka G, Vickers C, Willi O, Davies JR, Pukhov A and Meyerter-Vehn J (1999) Observation of collimated ionization channels in aluminum coated glass targets irradiated by ultraintense laser pulses. *Physical Review Letters* **83**, 4309.

Borghesi M, Mackinnon AJ, Campbell DH, Hicks DG, Kar S, Patel PK, Price D, Romagnani L, Schiavi A and Willi O (2004) Multi-MeV proton source investigations in ultraintense laser-foil interactions. *Physical Review Letters* **92**, 055003.

Bret A (2010) Collisional and collisionless beam plasma instabilities. *Laser and Particle Beams* **28**, 491–495.

Bret A, Fernandez MFJ and Anfray JM (2009) Unstable spectrum of a relativistic electron beam interacting with a quantum collisional plasma:

In conclusion, we have shown that self-resistive fields are very important to understand the transport of fast electron/ion beams, which can control the flow of mega-ampere currents in the intense laser-plasma interaction. This provides a direction to understand the instabilities arising at the interface of resistivity gradient targets that will otherwise lead to filamentation/pinching of the electron beams. Our experimental findings are in good agreement with the qualitative analysis performed using 2D PIC simulations. This offers a route to control and investigate these instabilities, which may otherwise prove detrimental for fast ignition experiments. Also, the magnetic fields of about 10^4 T are observed in the simulation, which may have implications in the

application to the Fast Ignition Scenario. *Plasma Physics and Controlled Fusion* **51**, 075011.

Cassam-Chenai G, Hughes JP, Reynoso EM, Badenes C and Moffett D (2008) Morphological evidence for azimuthal variations of the cosmic-ray ion acceleration at the blast wave of SN 1006. *The Astrophysical Journal* **680**, 1180–1197.

Chen H, Wilks SC, Bonlie JD, Liang EP, Myatt J, Price DF, Meyerhofer DD and Beiersdorfer P (2009) Relativistic positron creation using ultraintense short pulse lasers. *Physical Review Letters* **102**, 105001.

Clark EL, Krushelnick K, Davies JR, Zepf M, Tatarakis M, Beg FN, Machacek A, Norreys PA, Santala MIK, Watts I and Dangor AE (2000) Measurement of energetic transport through magnetized plasma from intense laser interactions with solids. *Physical Review Letters* **84**, 670.

Cowan TE, Perry MD, Key MH, Ditmire TR, Hatchett SP, Henry EA, Moody JD, Moran MJ, Pennington DM and Phillips TW (1999) High energy electrons, nuclear phenomena and heating in petawatt laser-solid experiments. *Laser and Particle Beams* **17**, 773.

Craxton RS, Anderson KS, Boehly TR, Goncharov VN, Harding DR, Knauer JP, McCrory RL, McKenty PW, Meyerhofer DD and Myatt JF (2015) Direct-drive inertial confinement fusion: a review. *Physics of Plasmas* **22**, 110501.

Davies JR, Bell AR, Haines MG and Guerin SM (1997) Short-pulse high-intensity laser-generated fast electron transport into thick solid targets. *Physical Review E* **56**, 7193.

Debayle A and Tikhonchuk VT (2008) Filamentation instability of a fast electron beam in a dielectric target. *Physical Review E* **78**, 066404.

Fried BD (1959) Mechanism for instability of transverse plasms waves. *Physics of Fluids* **2**, 337.

Fuchs J, Antici P, d'Humières E, Lefebvre E, Borghesi M, Brambrink E, Cecchetti CA, Kaluza M, Malka V, Manclossi M, Meyroneinc S, Mora P, Schreiber J, Toncian T, Pépin H and Audebert P (2006) Laser-driven proton scaling laws and new paths towards energy increase. *Nature Physics* **2**, 48.

Gahn C, Pretzler G, Saemann A, Tsakiris GD, Witte KJ, Gassmann D, Schätz T, Schramm U, Thirolf P and Habs D (1998) MeV γ-ray yield from solid targets irradiated with fs-laser pulses. *Applied Physics Letters* **73**, 3662.

Gahn C, Tsakiris GD, Pretzler G, Witte KJ, Delfin C, Wahlström CG and Habs D (2000) Generating positrons with fs-laser pulses. *Applied Physics Letters* **77**, 2662.

Grassi A, Grech M, Amiranoff F, Pegoraro F, Macchi A and Riconda C (2017) Electron Weibel instability in relativistic counter streaming plasmas with flow-aligned external magnetic fields. *Physical Review E* **95**, 023203.

Gremillet L, Amiranoff F, Baton SD, Gauthier JC, Koenig M, Martinolli E, Pisani F, Bonnaud G, Lebourg C, Rousseaux C, Toupin C, Antonicci A, Batani D, Bernardinello A, Hall T, Scott D, Norreys P, Bandulet H and Pepin H (1999) Time resolved observation of ultrahigh intensity laser-produced electron jets propagating through transparent solid targets. *Physical Review Letters* **83**, 5015.

Gremillet L, Bonnaud G and Amiranoff F (2002) Filamented transport of laser-generated relativistic electrons penetrating a solid target. *Physics of Plasmas* **9**, 941.

Jung R, Osterholz J, Wenbrück KL, Kiselev S, Pretzler G, Pukhov A, Willi O, Kar S, Borghesi M, Nazarov W, Karsch S, Clarke R and Neely D (2005) Study of electron-beam propagation through preionized dense foam plasma. *Physical Review Letters* **94**, 195001.

Kar S, Markey K, Simpson PT, Bellei C, Green JS, Nagel SR, Kneip S, Carroll DC, Dromey B, Willingale L, Clark EL, McKenna P, Najmudin Z, Krushelnick K, Norreys P, Clarke RJ, Neely D, Borghesi M and Zepf M (2008) Dynamic control of laser-produced proton beams. *Physical Review Letters* **100**, 105004.

Kar S, Markey K, Borghesi M, Carroll DC, McKenna P, Neely D, Quinn MN and Zepf M (2011) Ballistic focussing of polyenergetic protons driven by petawatt laser pulses. *Physical Review Letters* **106**, 225003.

Krasheninnikov SI, Kim AV, Frolov BK and Stephens R (2005) Intense electron beam propagation through insulators: ionization front structure and stability. *Physics of Plasmas* **12**, 073105.

Ledingham KWD, Spencer I, McCanny T, Singhal RP, Santala MIK, Clark E, Watts I, Beg FN, Zepf M and Krushelnick K (2000) Photonuclear physics when a multiterrawatt laser pulse interacts with solid targets. *Physical Review Letters* **84**, 899.

Maksimchuk A, Gu S, Flippo K, Umstadter D and Yu Bychenkov V (2000) Forward ion acceleration in thin films driven by a high-intensity laser. *Physical Review Letters* **84**, 4108.

Metzkes J, Kluge T, Zeil K, Bussmann M, Kraft SD, Cowan TE and Schramm U (2014) Experimental observation of transverse modulations in laser-driven proton beams. *New Journal of Physics* **16**, 023008.

Mora P (2003) Plasma expansion into a vacuum. *Physical Review Letters* **90**, 185002.

Nishiuchi M, Daito I, Ikegami M, Daido H, Mori M, Orimo S, Ogura K, Sagisaka A, Yogo A, Pirozhkov AS, Sugiyama H, Kiriyama H, Okada H, Kanazawa S, Kondo S, Shimomura T, Tanoue M, Nakai Y, Sasao H, Wakai D, Sakaki H, Bolton P, Choi IW, Sung JH, Lee J, Oishi Y, Fujii T, Nemoto K, Souda H, Noda A, Iseki Y and Yoshiyuki T (2009) Focussing and spectral enhancement of a repetition-rated, laser-driven, divergent multi-MeV proton beam using permanent quadrupole magnets. *Applied Physics Letters* **94**, 061107.

Norreys PA, Santala M, Clark E, Zepf M, Watts I, Beg FN, Krushelnick K, Tatarakis M, Dangor AE and Fang X (1999) Observation of highly directional γ-ray beam from ultrashort, ultraintense laser pulse interactions with solids. *Physics of Plasmas* **6**, 2150.

Ramakrishna B, Kar S, Robinson APL, Adams DJ, Markey K, Quinn MN, Yuan XH, McKenna P, Lancaster KL, Green JS, Scott RHH, Norreys PA, Schreiber J and Zepf M (2010) Laser-driven fast electron collimation in targets with resistivity boundary. *Physical Review Letters* **105**, 135001.

Ramakrishna B, Tayyab M, Bagchi S, Mandal T, Upadhyay A, Weng SM, Murakami M, Cowan TE, Chakera JA, Naik PA and Gupta PD (2015) Filamentation control and collimation of laser accelerated MeV protons. *Plasma Physics and Controlled Fusion* **12**, 125013.

Robinson APL and Sherlock M (2007) Magnetic collimation of fast electrons produced by ultraintense laser irradiation by structuring the target composition. *Physics of Plasmas* **14**, 083105.

Robinson APL, Kingham RJ, Ridgers CP and Sherlock M (2008) Effect of transverse density modulations on fast electron transport in dense plasmas. *Plasma Physics and Controlled Fusion* **50**, 065019.

Robson L, Simpson PT, McKenna P, Ledingham KWD and Clarke RJ (2006) Scaling of proton acceleration driven by petawatt laser-plasma interactions. *Nature Physics* **3**, 58.

Romagnani L, Robinson APL, Clarke RJ, Doria D, Lancia L, Nazarov W, Notley MM, Pipahl A, Quinn K, Ramakrishna B, Wilson PA, Fuchs J, Willi O and Borghesi M (2019) Dynamics of the electromagnetic fields induced by fast electron propagation in near-solid-density media. *Physical Review Letters* **122**, 025001.

Sakagami H, Johzaki T, Sunahara A and Nagatomo H (2016) Integrated simulations for ion beam assisted fast ignition. *Journal of Physics: Conference Series* **1688**, 012096.

Santala MIK, Zepf M, Watts I, Beg FN, Clark E, Tatarakis M, Krushelnick K, Dangor AE, McCanny T, Spencer I, Singhal RP, Ledingham KWD, Wilks SC, Machacek AC, Wark JS, Allott R, Clarke RJ and Norreys PA (2000) Effect of the plasma density scale length on the direction of fast electrons in relativistic laser-solid interactions. *Physical Review Letters* **84**, 1459.

Schramm U, Bussmann M, Irman A, Siebold M, Zeil K, Albach D, Bernert C, Bock S, Brack F and Branco J (2017) First results with the novel petawatt laser acceleration facility in Dresden. *Journal of Physics: Conference Series* **874**, 012028.

Sentoku Y, Mima K, Kojima S and Ruhi H (2000) Magnetic instability by the relativistic laser pulses in overdense plasmas. *Physics of Plasmas* **7**, 689.

Sentoku Y, d'Humieres E, Romagnani L, Audebert P and Fuchs J (2011) Dynamic control over mega-ampere electron currents in metals using ionization-driven resistive magnetic fields. *Physical Review Letters* **107**, 135005.

Snavely RA, Key MH, Hatchett SP, Cowan TE, Roth M, Phillips TW, Stoyer MA, Henry EA, Sangster TC and Singh MC (2000) Intense high energy proton beams from petawatt laser-irradiation of solids. *Physical Review Letters* **85**, 2945.

Strickland D and Mourou G (1985) Compression of amplified chirped pulses. *Optics Communications* **55**, 447.

Suzuki-Vidal F (2015) How to spark a field. *Nature Physics* **11**, 98–99.

Tatarakis M, Beg FN, Clark EL, Dangor AE, Edwards RD, Evans RG, Goldsack TJ, Ledingham KWD, Norreys PA, Sinclair MA, Wei MS, Zepf M and Krushelnick K (2003) Propagation instabilities of high-intensity laser-produced electron beams. *Physical Review Letters* **90**, 175001.

Toncian T, Borghesi M, Fuchs J, d'Humieries E, Antici P, Audebert P, Brambrink E, Cecchetti CA, Pipahl A, Romagnani L and Willi O (2006) Ultrafast laser-driven microlens to focus and energy select Mega-Electron Volt protons. *Science* **312**, 410.

Wei MS, Beg FN, Clark EL, Dangor AE, Evans RG, Gopal A, Ledingham KWD, McKenna P, Norreys PA, Tatarakis M, Zepf M and Krushelnick K (2004) Observations of the filamentation of high-intensity laser-produced electron beams. *Physical Review E* **70**, 056412.

Weibel ES (1959) Spontaneously growing transverse waves in a plasma due to an anisotropic velocity distribution. *Physical Review Letters* **2**, 83.

Xu XH, Liao Q, Wu MJ, Geng YX, Li DY, Zhu JG, Li CC, Hu RH, Shou YR, Chen YH, Lu HY, Ma WJ, Zhao YY, Zhu K, Lin C and Yan XQ (2019) Detection and analysis of laser driven proton beams by calibrated Gafchromic HD-V2 and MD-V3 radiochromic films. *Review of Scientific Instruments* **90**, 033306.

Yu J, Jiang Z, Kieffer JC and Krol A (1999) Hard x-ray emission in high intensity femtosecond laser-target interaction. *Physics of Plasmas* **6**, 1318.